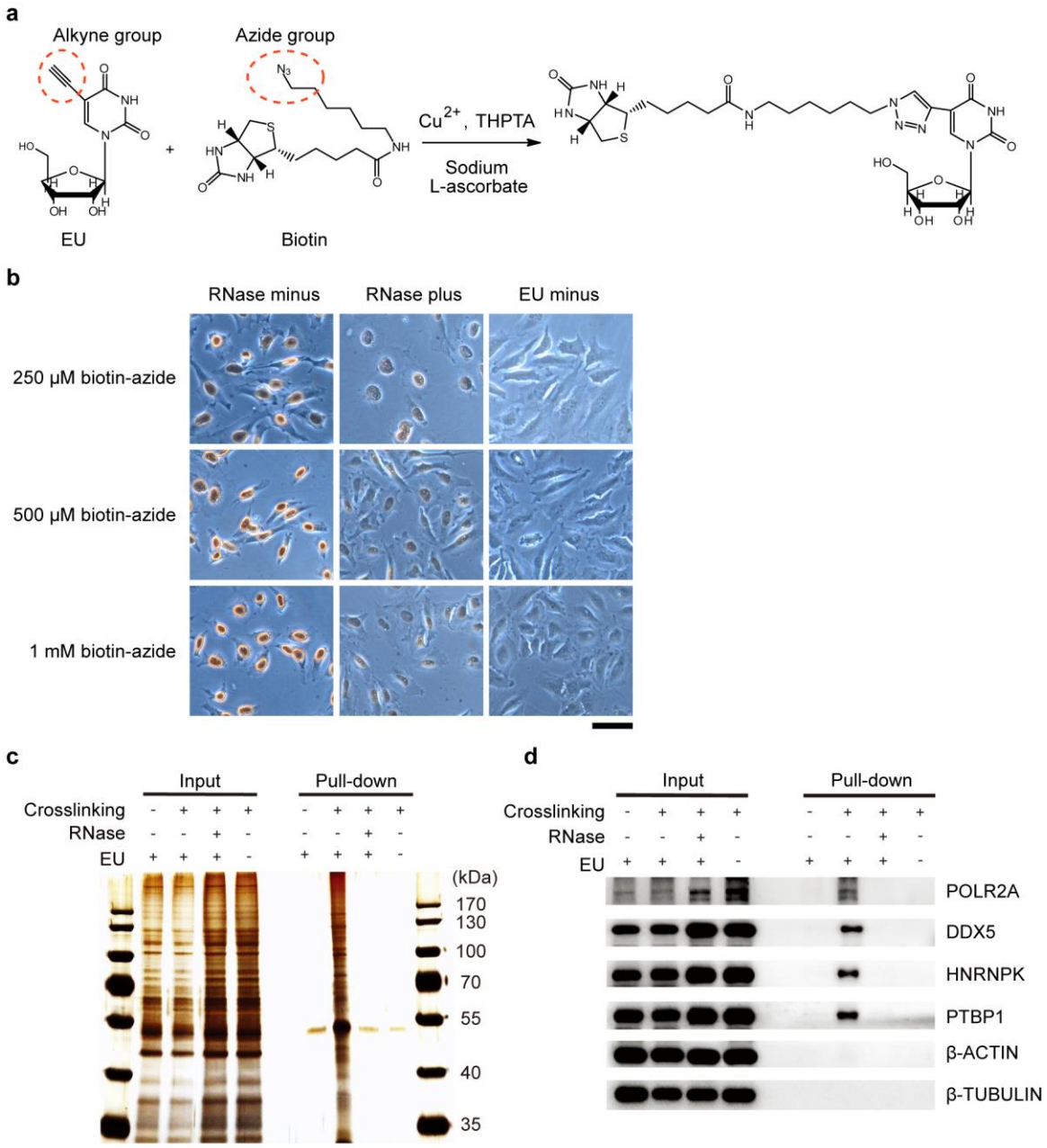

Supplementary Figure 1

EU labeling and protein capture using RICK**.**

a, Schematic showing the conjugation of a biotin-azide to the nucleoside analog EU (incorporated into RNA) by click chemistry; Cu^{2+} and sodium L-ascorbate were used as catalysts, and tris(3-hydroxypropyltriazolylmethyl)amine (THPTA) as ligand. **b**, Visualization of EU incorporation (indicated by horseradish peroxidase activity using DAB staining) in HeLa cells. RNase A and different concentrations of biotin-azide were added as indicated. Scale bar, 100 μm; 3 biologically independent experiments were performed. (**c**-**d**), Silver staining (**c**) and Western blotting (**d**) of proteins eluted from a representative RICK experiment of HeLa cells labeled with EU for 16 hours. β-ACTIN and β-TUBULIN were used as negative controls, and POLR2A, DDX5, HNRNPK, and PTBP1 as positive controls; 3 biologically independent experiments were performed.

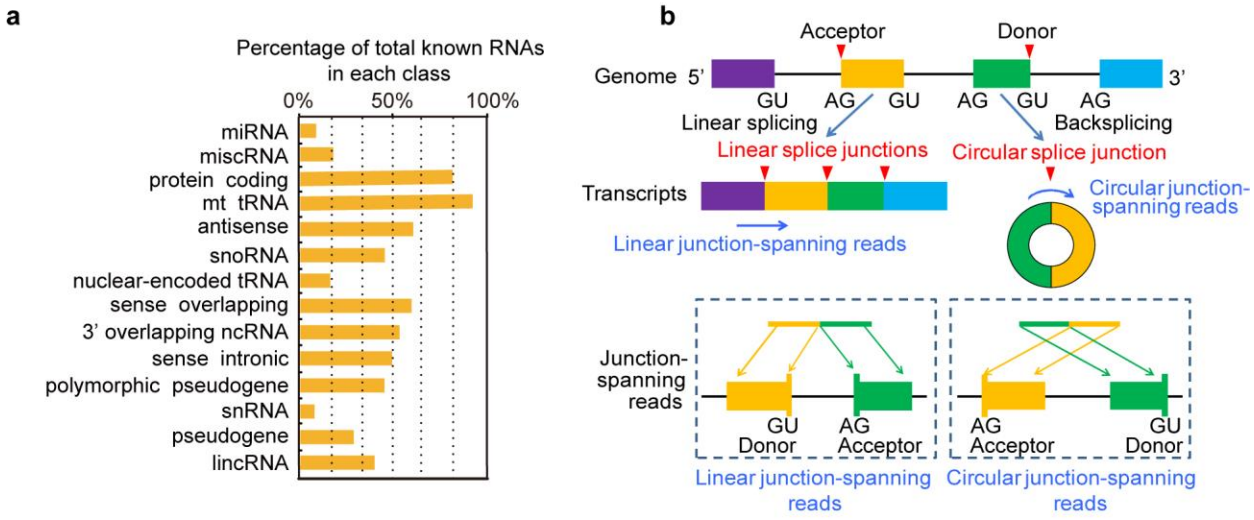

c

Name	Coding gene	Read No. RICK/oligo(dT)	Sequence of joint site
Circ-6763	*CCAT1*	92/0	CCAGGTTGGG ATTAGCAATG
Circ-1903	*RPPH1*	23/0	GCCAGCGAAG GTGAGTTCCC
Circ-2154	*MGA*	14/0	TTTCTGAATG GGATGGGAAG
Circ-1557	*CPSF6*	10/0	TCGTTAGAAG GGAAGCTGAA
Circ-2327	*IGF1R*	7/0	TGCCAGAAAA GTCTGCGGGC
Circ-3811	*TET3*	2/0	GATTGCGTCG GACAGGCTCA

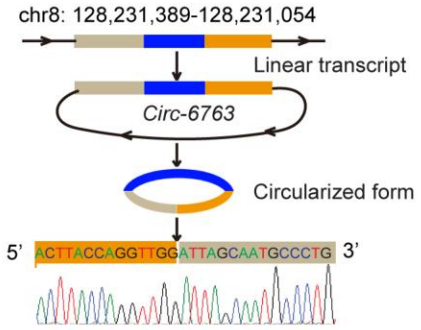

Supplementary Figure 2

Analysis of circRNAs isolated by RICK**.**

a, RNA species isolated by RICK. The percentage of total known RNAs in each class was calculated according to Ensemble annotations. **b**, Workflow showing the methodology used for circRNA identification. **c**, Representative candidate circRNAs identified by RICK; 2 biologically independent experiments were performed. **d**, Sanger sequencing of a representative circRNA to confirm its sequence; 2 biologically independent experiments were performed.

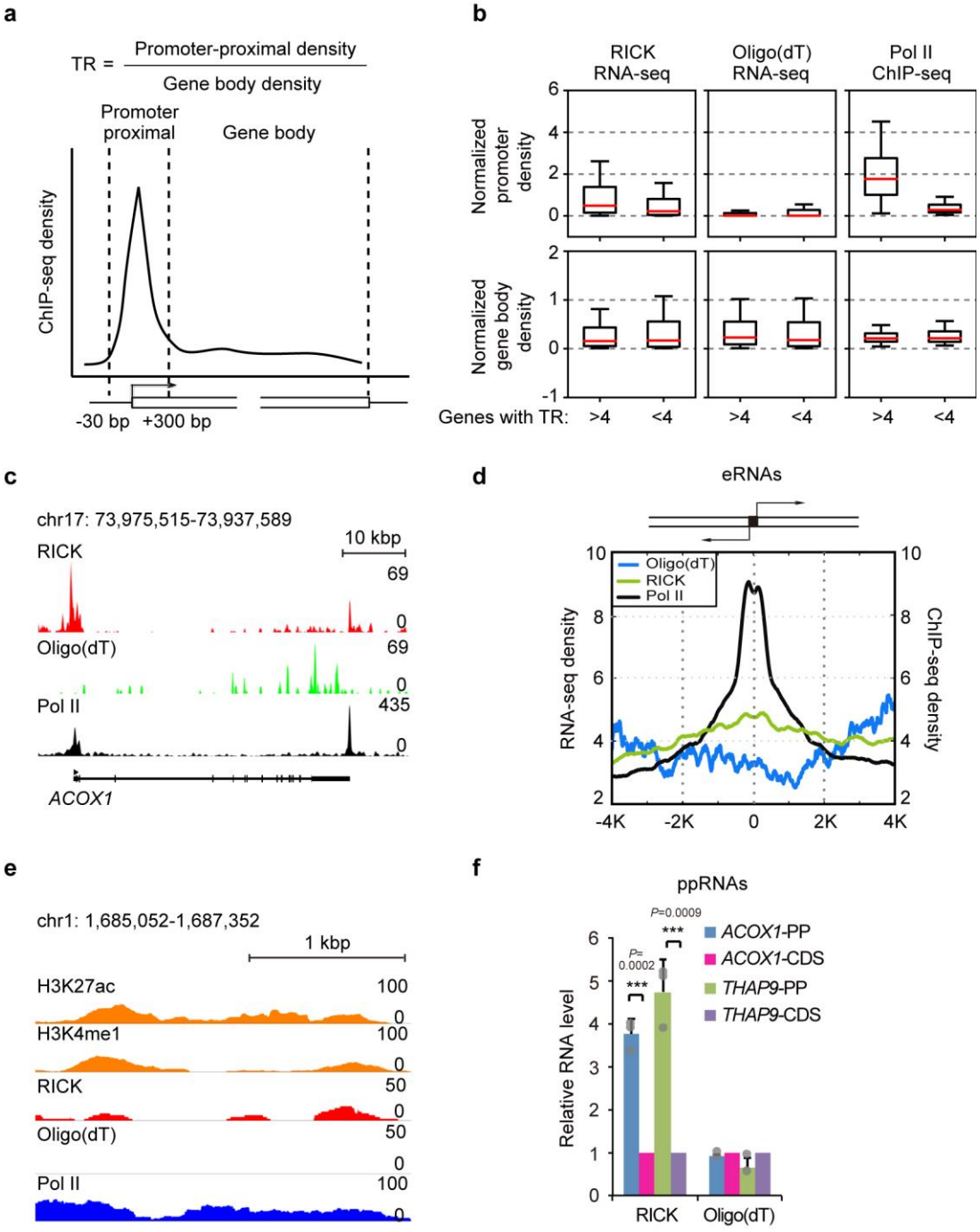

Supplementary Figure 3

Analysis of ppRNAs and eRNAs isolated by RICK.

a, Schematic showing the calculation used to determine the Pol II TR. **b**, Normalized gene body and promoter density of either RICK or oligo(dT) RNA-seq peaks[1]; Pol II occupancy[16] was used to categorize different gene classes based on their TR, TR>4 (n=5,889) and TR<4 (n=6,838). The central line is the median, the boxes indicate the upper and lower quartiles, the whiskers indicate 1.5 × interquartile range. **c**, Pol II ChIP-seq peaks and RICK/oligo(dT) RNA-seq peaks for the *ACOX1* gene locus. **d**, Metagene representation of Pol II (black) occupancy and RICK (green)/oligo(dT) (blue) RNA-seq intensity at loci producing eRNAs identified by

FANTOM5 database[17]; n=2,189. **e**, H3K27ac and H3K4me1[40], Pol II ChIP-seq peaks, and RICK/oligo(dT) RNA-seq peaks at a specific enhancer site. One representative experiment is shown; n=2 biologically independent RICK samples were sequenced and analyzed. **f**, RT-qPCR analysis of ppRNAs and elongated RNAs for 2 representative genes with paused Pol II in both RICK and oligo(dT) capture samples. Relative RNA levels were first normalized to the input and then to the coding DNA sequence; n=3 biologically independent experiments and data are shown as the mean ± SD. PP indicates promoter-proximal and CDS coding DNA sequence, respectively. *P* value is shown (Student's *t*-test, two tailed).

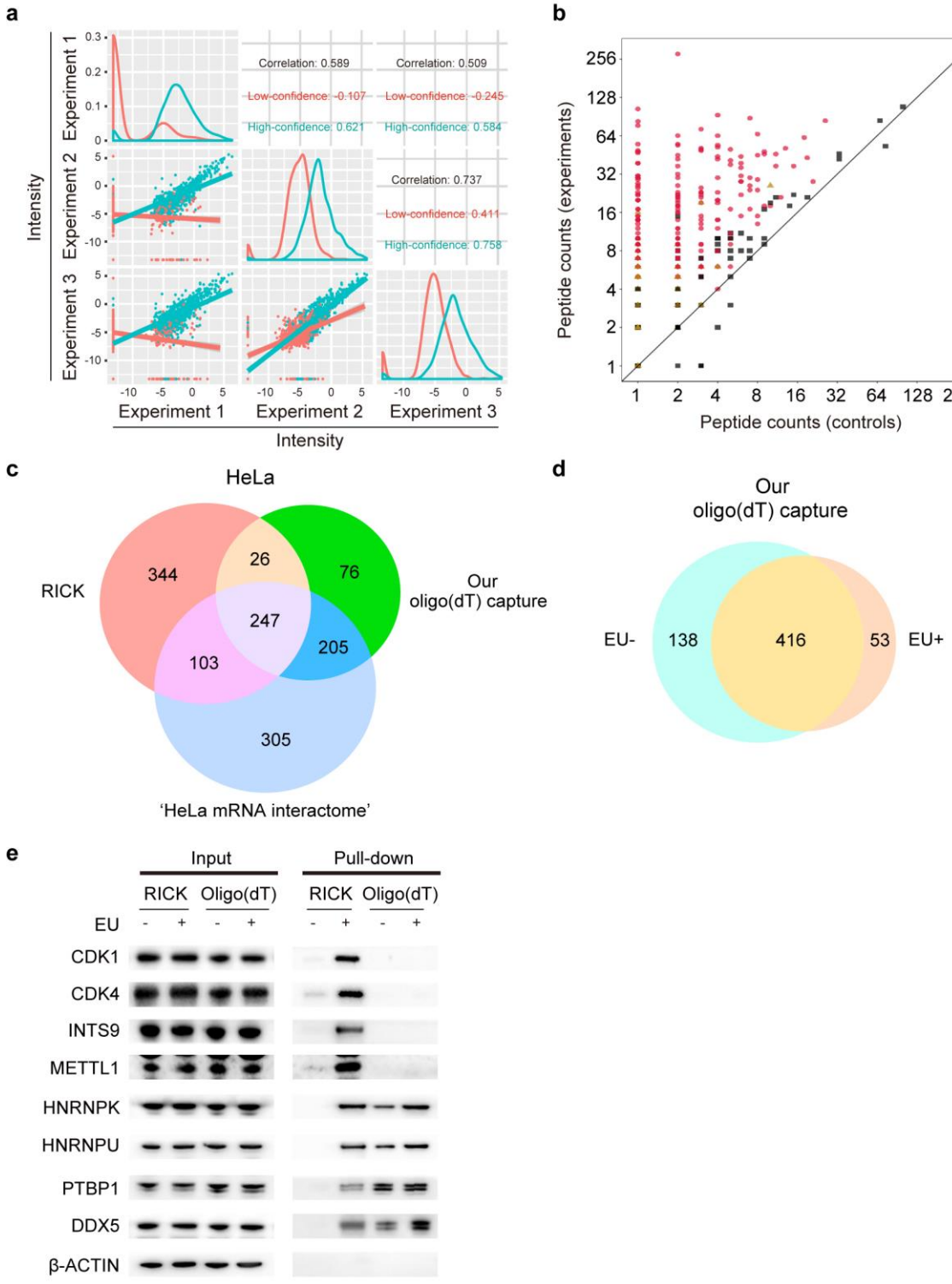

Supplementary Figure 4

Proteins identified by RICK.

a, Correlation analysis of LC-MS/MS in 3 independent RICK experiments. 'Correlation' indicates the pairwise Pearson correlation of all 1,353 identified proteins, 'high-confidence' represents the 720 high-confidence proteins, and 'low-confidence' the 633 low-confidence

proteins. Both X-axis and Y-axis in scatter plots are ion intensities. Curves show the intensity distribution of 'high-confidence proteins' (cyan) and 'low-confidence proteins' (red) in each experiment. Solid straight cyan and solid straight red trend lines represent linear regression of high-confidence and low-confidence proteins, respectively. **b**, Scatter plot showing the comparison of unique peptide counts in both control and RICK experiment groups; the circles indicate 'high-confidence proteins', the triangles indicate 'low-confidence proteins', and the squares indicate 'background proteins'. **c**, Venn diagram comparing the high-confidence proteins identified by RICK, the 'HeLa mRNA interactome'[1], and our own oligo(dT) capture without EU treatment. **d**, Venn diagram comparing the proteins identified by oligo(dT) capture of HeLa cells cultured with or without EU for 16 hours. **e**, Representative Western blot detecting the capture of selected proteins identified by RICK and oligo(dT) capture with or without EU. β-ACTIN was used as a negative control, and HNRNPK, HNRNPU, PTBP1, and DDX5 as positive controls; 3 biologically independent experiments were performed.

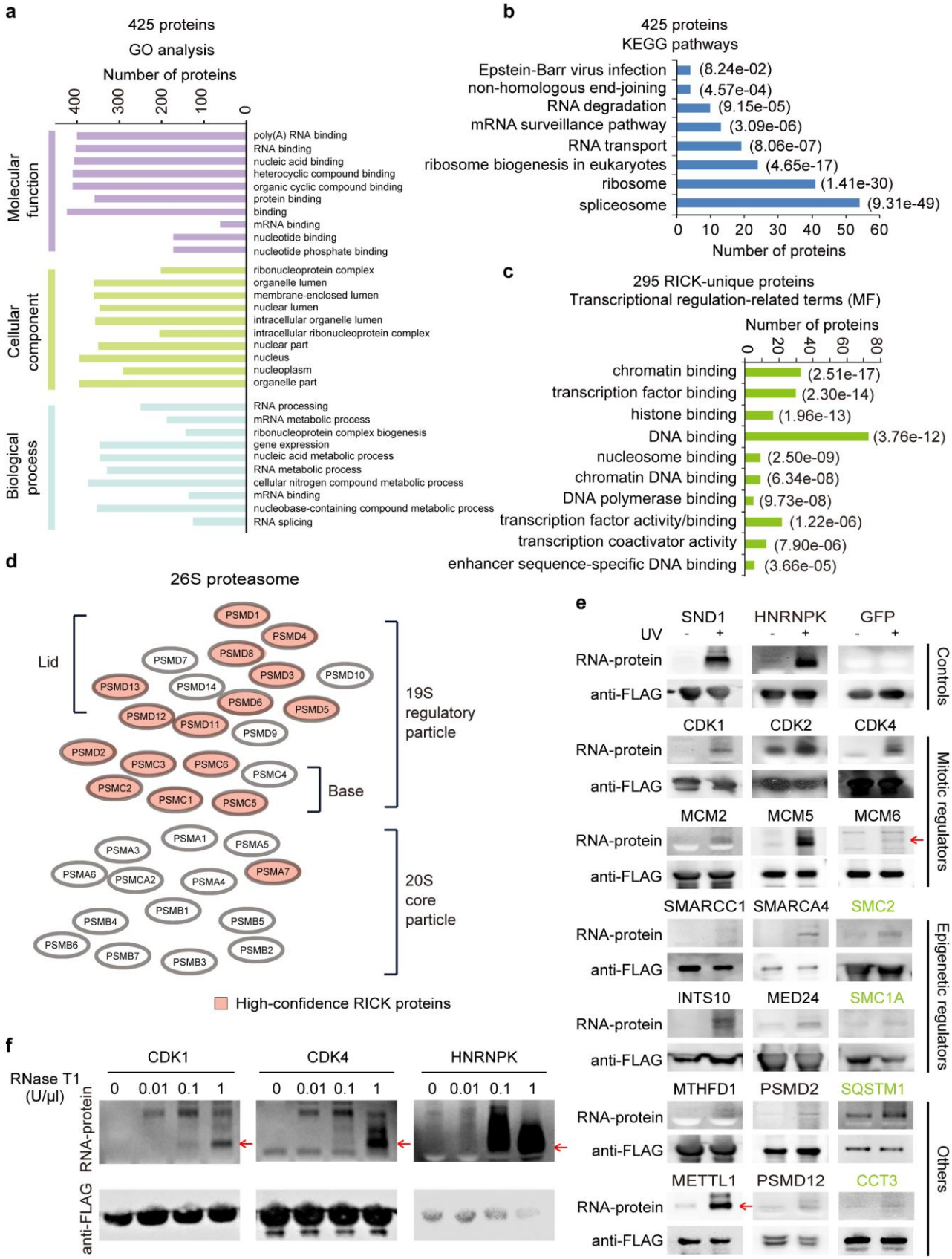

Nature Methods: doi:10.1038/nmeth.4595

Supplementary Figure 5

Functional characterization of proteins overlapping in RICK and oligo(dT) capture.

a, GO analysis for the 425 proteins identified by RICK and present in different oligo(dT) capture datasets[1,2,18,19]; the top 10 GO terms with the smallest *P* value in the indicated categories are shown. The number of proteins for each individual term is also shown. *P* value is also shown (Fisher's exact test, one tailed). **b**, KEGG pathway analysis of the 425 proteins identified by RICK and present in different oligo(dT) capture datasets. The number of proteins for each individual pathway is also shown. The numbers in the parentheses are *P* values (Fisher's exact test, one tailed). **c**, GO terms belonging to the molecular functions (MF) category that are related to transcriptional regulation in the 295 RICK-unique RBPs. The number of proteins for each individual term is also shown. **d**, Schematic representation of the proteasome complex, the subunits identified by RICK are shown in red (high-confidence group) or blue (low-confidence group). **e**, RNA binding activity of selected proteins from the 344 RICK-exclusive RBPs was detected by PAR-CLIP-biotin chemiluminescent nucleic acid detection. Proteins related to mitosis, epigenetic regulation, and others were selected. Antibodies against FLAG were used to confirm the protein size and equal loading of samples. GFP was used as a negative control, SND1 and HNRNPK as positive controls. We also used SMC2, SMC1A, SQSTM1 and CCT3 (in green), identified by our own or other oligo(dT) capture study by Baltz *et al*.[2], as additional positive controls. Arrowheads indicate specific bands. Representative gels are shown, 3 biologically independent experiments were performed. **f**, Representative PAR-CLIP-biotin chemiluminescent nucleic acid detection showing the RNA binding activities of CDK1, CDK4, and HNRNPK (positive control) in the presence of different RNase T1 concentrations. Western blotting was used to confirm protein size and comparable loading of samples. Arrowheads indicate specific bands; 3 biologically independent experiments were performed.

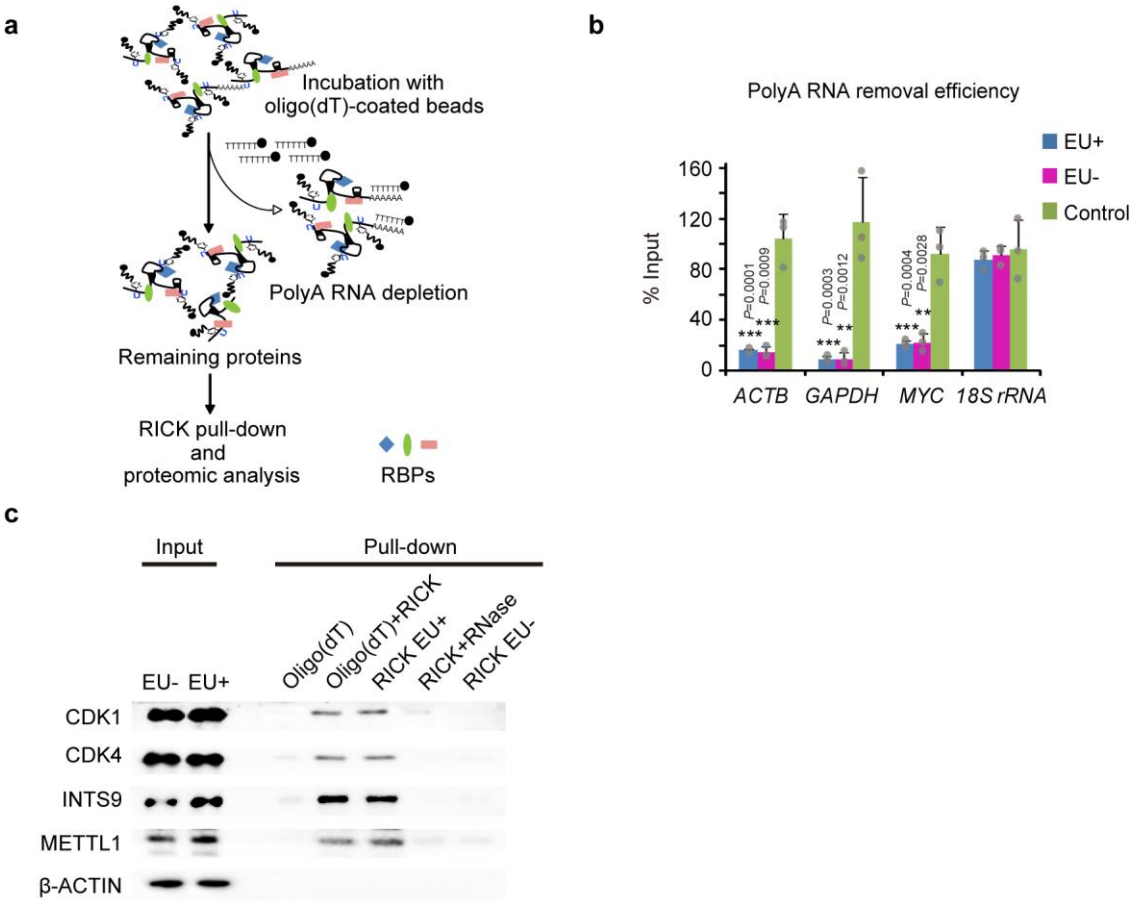

Supplementary Figure 6

PolyA-depleted RICK identifies proteins with preferential binding to non-polyA RNAs

a, Schematic showing the polyA-depleted RICK protocol. **b**, RT-qPCR to confirm the polyA RNA removal efficiency. 'Control' indicates samples after incubation with control beads (no oligo(dT)-coating), 'EU+/-' indicate samples (with/without EU) after incubation with oligo(dT) beads. *18S rRNA* was used as a non-polyA RNA control; n=3 biologically independent experiments and data are shown as the mean ± SD. *P* value is shown (Student's *t*-test, two tailed). **c**, Representative Western blots showing the isolation of selected proteins (CDK1, CDK4, INTS9, and METTL1) by RICK and polyA-depleted RICK, but not by RICK with RNase treatment, oligo(dT) capture, or RICK without EU treatment (negative control); 3 biologically independent experiments were performed.

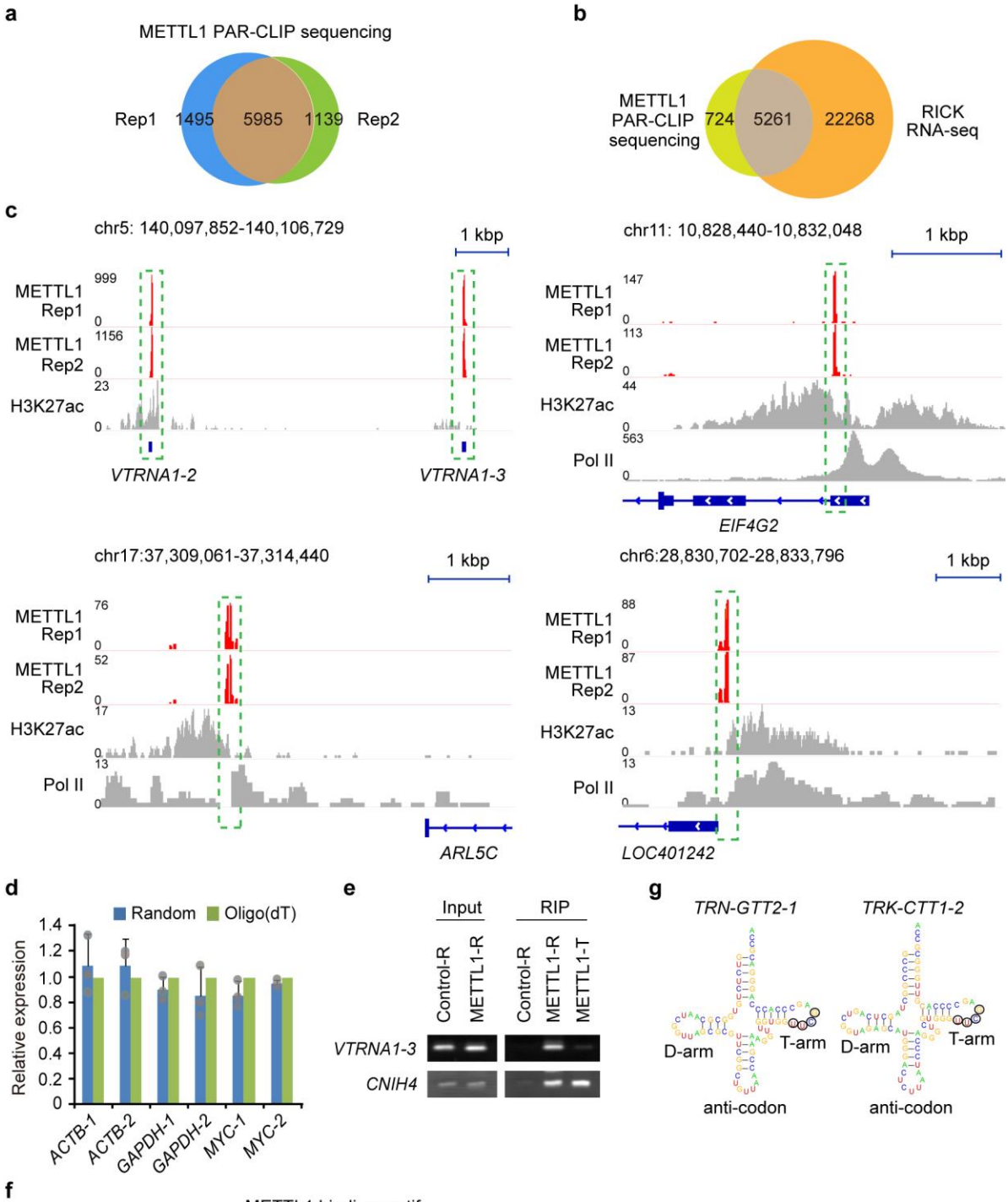
a
METTL1 PAR-CLIP sequencing
Rep1
1495
5985
1139
Rep2
b
METTL1 PAR-CLIP sequencing
724
5261
22268
RICK RNA-seq
c
chr5: 140,097,852-140,106,729
1 kbp
METTL1 Rep1
METTL1 Rep2
H3K27ac
VTRNA1-2
VTRNA1-3
chr11: 10,828,440-10,832,048
1 kbp
METTL1 Rep1
METTL1 Rep2
H3K27ac
Pol II
EIF4G2
chr17:37,309,061-37,314,440
1 kbp
METTL1 Rep1
METTL1 Rep2
H3K27ac
Pol II
ARL5C
chr6:28,830,702-28,833,796
1 kbp
METTL1 Rep1
METTL1 Rep2
H3K27ac
Pol II
LOC401242
d
Random
Oligo(dT)
Relative expression
ACTB-1
ACTB-2
GAPDH-1
GAPDH-2
MYC-1
MYC-2
e
Input
RIP
Control-R
METTL1-R
Control-R
METTL1-R
METTL1-T
VTRNA1-3
CNIH4
g
TRN-GTT2-1
TRK-CTT1-2
D-arm
T-arm
anti-codon
D-arm
T-arm
anti-codon
f
METTL1 binding motif
Non-tRNA group
tRNA group
Rep1
p=1e-203
p=1e-908
Rep2
p=1e-174
p=1e-811

Supplementary Figure 7

Identification of METTL1-bound RNAs.

a, Venn diagram comparing the transcripts identified by 2 independent METTL1 PAR-CLIP sequencing experiments. **b**, Venn diagram comparing the transcripts identified with METTL1 PAR-CLIP sequencing and RICK RNA-seq. **c**, Track view of METTL1 PAR-CLIP sequencing data showing regions at the *VTRNA1-2* and *VTRNA1-3* loci, the *EIF4G2* locus, the regions proximal to *ARL5C* and the regions proximal to the *LOC401242* locus. H3K27ac[40] and Pol II[16] signals are also shown; n=2 biologically independent PAR-CLIP sequencing were analyzed. **d**, Comparison of the efficiency of reverse transcription of the selected oligo(dT)-captured mRNAs using random hexamers or oligo(dT) primers; 2 pairs of amplification primers for each individual gene were used for qPCR; n=3 biologically independent experiments and data are shown as the mean ± SD. **e**, Semi-quantitative PCR analysis of selected METTL1-bound RNAs. Random hexamers or oligo(dT) primers were used as indicated for the reverse transcription; n=2 biologically independent experiments were performed. **f**, METTL1 binding motifs on non-tRNA (n=25,751 and 20,367 for Rep1 and Rep2, respectively) or tRNA groups (n=1,022 and 858 for Rep1 and Rep2, respectively) identified in 2 independent PAR-CLIP sequencing experiments. *P* value is shown (Fisher's exact test, one tailed). **g**, Representative METTL1-bound tRNAs are shown; the 'UUCG' core sequence on the T arm are marked with circles.

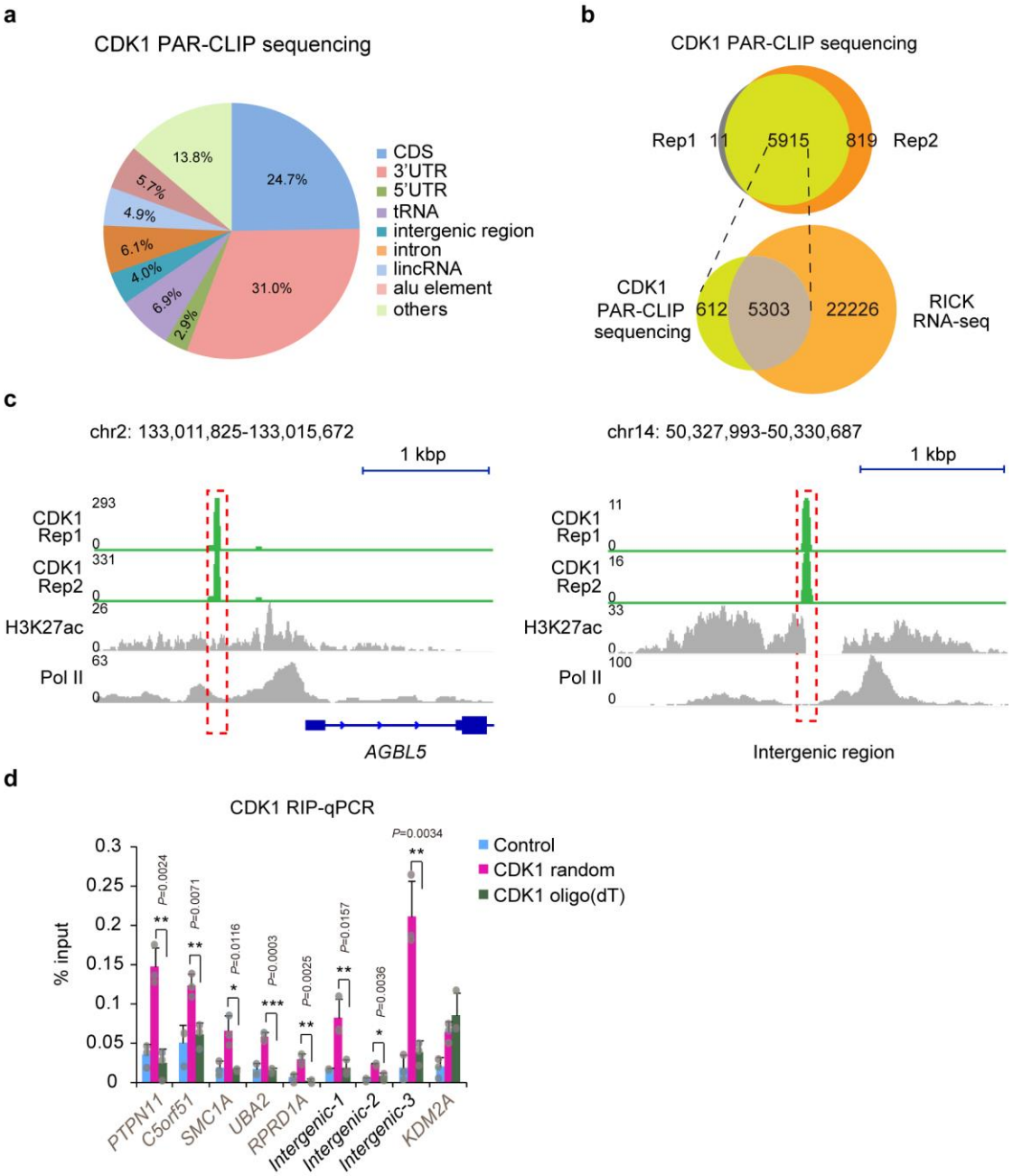

Supplementary Figure 8

Identification of CDK1-binding RNAs.

a, Distribution of RNA species identified by CDK1 PAR-CLIP sequencing. The average of n=2 biologically independent experiments is shown. **b**, Venn diagram comparing the transcripts identified with CDK1 PAR-CLIP sequencing and RICK RNA-seq. **c**, Track view of CDK1 PAR-CLIP sequencing data showing regions proximal to *AGBL5* (left panel) and at an intergenic locus (right panel); n=2 biologically independent PAR-CLIP sequencing were analyzed. **d**, RIP-qPCR analysis of different RNAs binding to CDK1 identified in the PAR-CLIP sequencing. The enrichments were normalized to input; GFP was used as negative control. Random hexamers or oligo(dT) primers were used for the reverse transcription as indicated. CDK1-interacting mRNAs are marked in grey as opposed to intergenic RNAs; n=3 biologically independent experiments and data are shown as the mean ± SD. *P* value is shown (Student's *t*-test, two tailed).

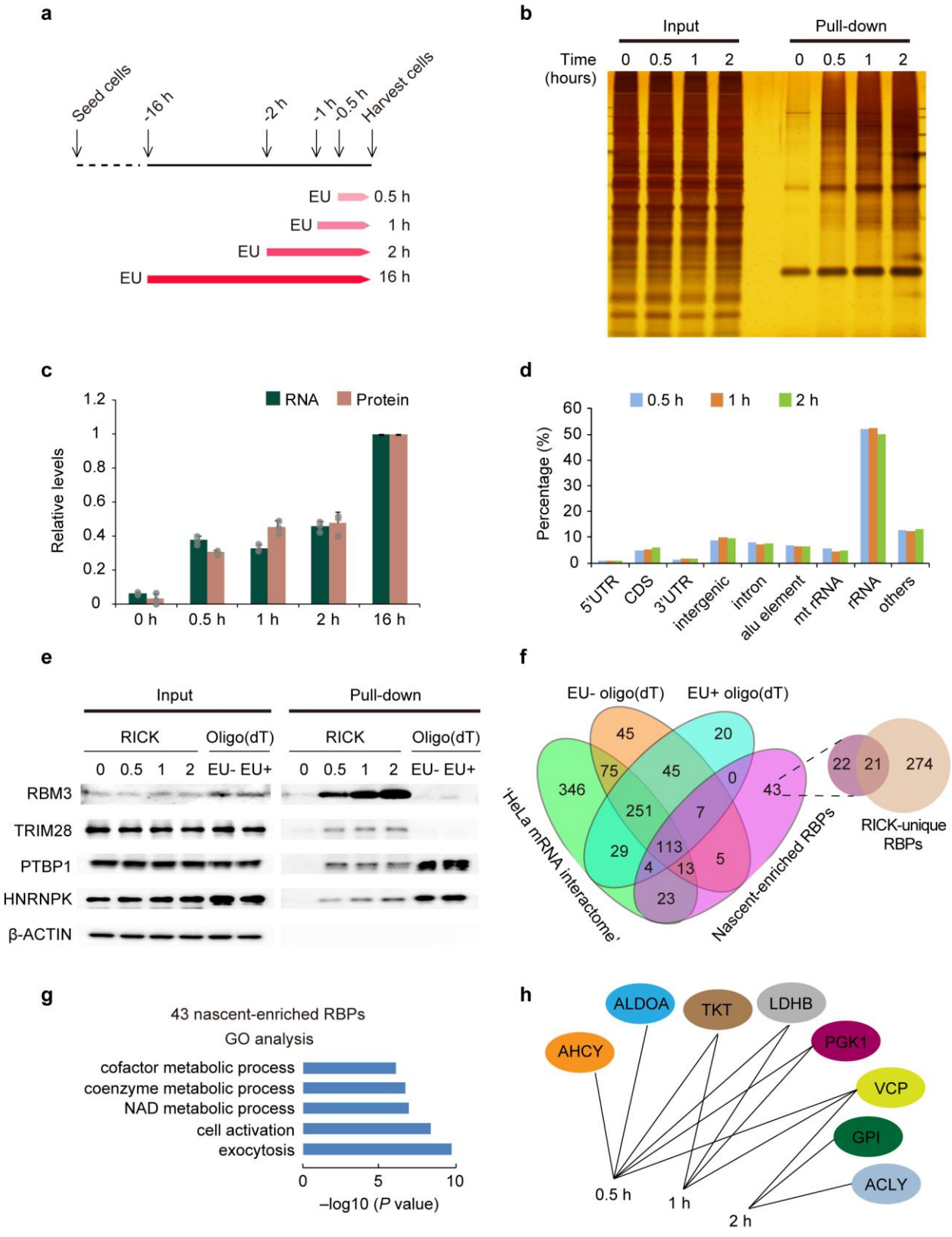

Supplementary Figure 9

Capture of the nascent-enriched RNA interactome in HeLa cells.

a, Schematic diagram showing procedures of 16-hour RICK and short labeling RICK. **b**, Silver staining of proteins eluted from representative RICK experiments of HeLa cells with short EU labeling times; n=3 biologically independent experiments were performed. **c**, Relative levels of RNA and protein isolated by RICK with short EU labeling time points compared to 16-hour RICK; n=3 biologically independent experiments and data are shown as the mean ± SD. **d**, Distribution of RNA species isolated in RICK experiments with short EU labeling times (0.5, 1, and 2 h); One experiment was performed; h indicates hour. **e**, Representative Western blot confirming the capture of 2 selected proteins identified by RICK with short EU labeling times in contrast to oligo(dT) capture with or without EU. PTBP1 and HNRNPK were detected in both short labeling RICK and oligo(dT) capture samples. β-ACTIN was used as a negative control; 3 biologically independent experiments were performed. **f**, Venn diagram comparing the 208 nascent-enriched RBPs with 'HeLa mRNA interactome' and our oligo(dT) capture in HeLa with or without EU (left); Venn diagram comparing the 43 nascent-enriched RBPs with the 295 RICK-unique RBPs (right). **g**, GO analysis (biological process) for the 43 nascent-specific RBPs; *P* value for the indicated categories is shown. (Fisher's exact test, one tailed). **h**, Metabolic enzymes/factors isolated by short labeling RICK and absent in the 'HeLa mRNA interactome'[1] or our own oligo(dT) capture dataset.

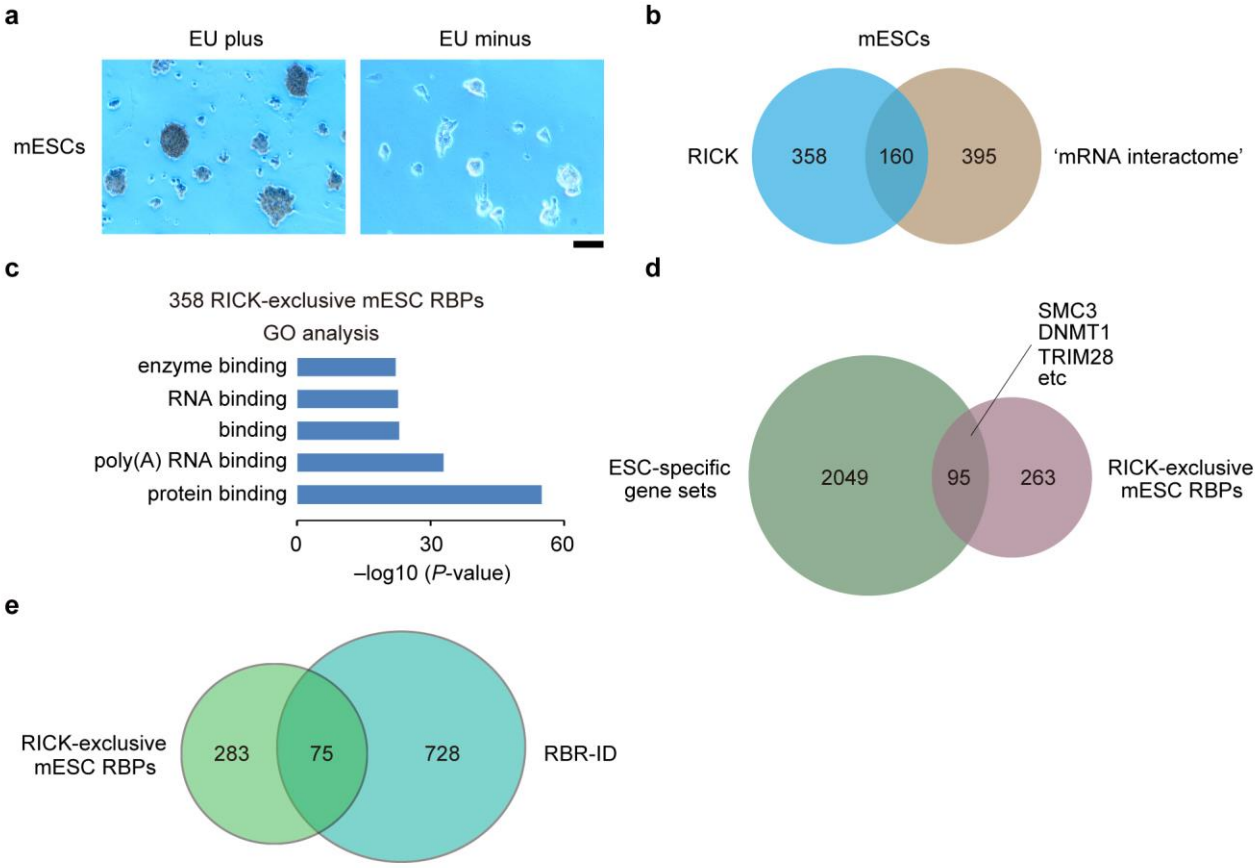

Supplementary Figure 10

Application of RICK to mESCs.

a, Visualization of EU incorporation (indicated by horseradish peroxidase activity) in mESCs. Scale bar, 100 μm; n=2 biologically independent experiments were performed. **b**, Venn diagram comparing the RICK-identified RBPs in mESCs with the 'mESC mRNA interactome'. **c**, GO analysis of the RICK-exclusive mESC RBPs; *P* value in the indicated categories is shown (Fisher's exact test, one tailed). **d**, Venn diagram comparing the RICK-exclusive mESC RBPs with the 'ESC-specific gene sets'[29-32]; The 'ESC-specific gene sets' is a combination of different gene sets in human embryonic stem cell and mESC studies. **e**, Venn diagram comparing the RICK-exclusive mESC RBPs with RBR-ID-identified proteins.

Supplementary Fig. 1c

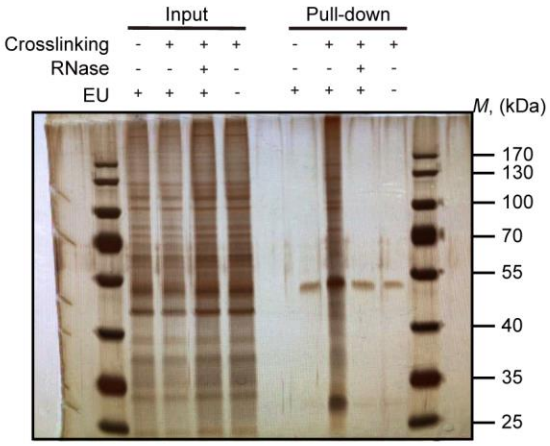

Supplementary Fig. 1d

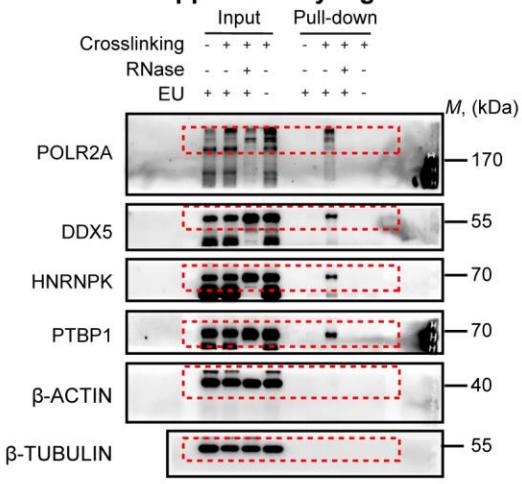

Supplementary Fig. 4e

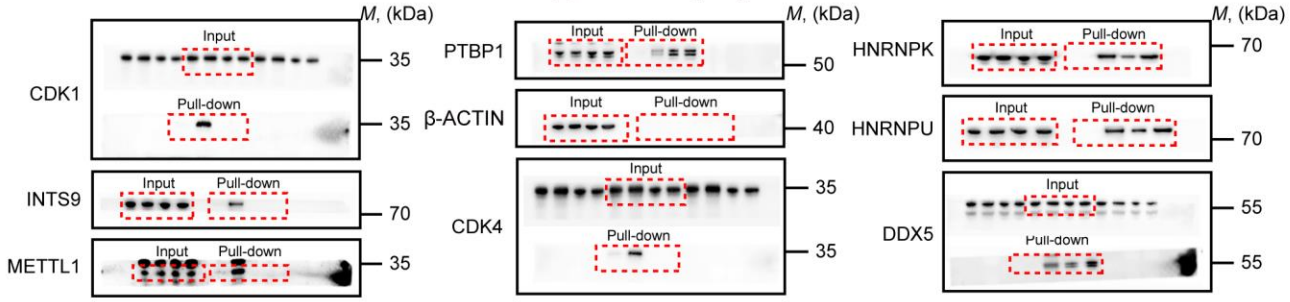

Supplementary Fig. 5e

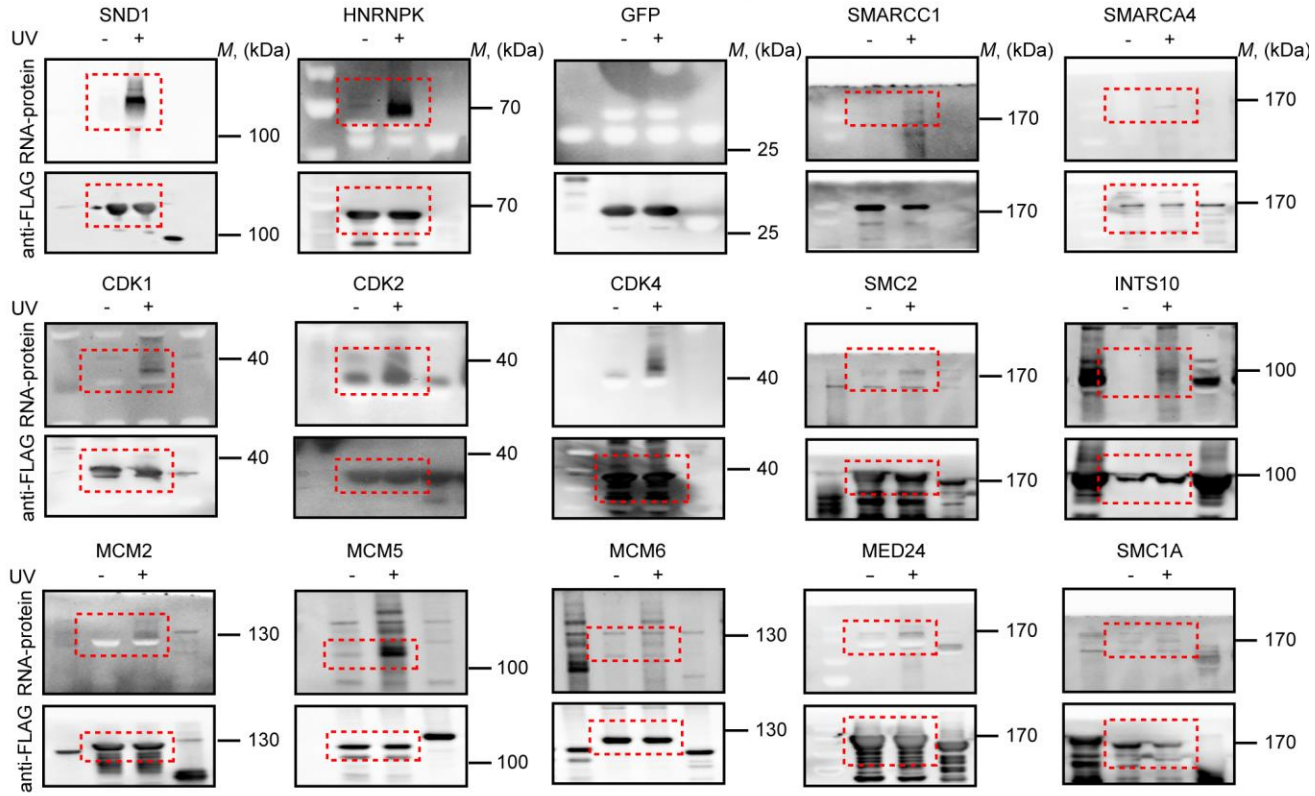

Nature Methods: doi:10.1038/nmeth.4595

Supplementary Figure 11

Raw gels for all figures in the manuscript.

All the gels used in this manuscript have been repeated independently at least 3 times in our laboratory. This figure shows the original scans for all of the representative gels.

Supplementary Fig. 5e

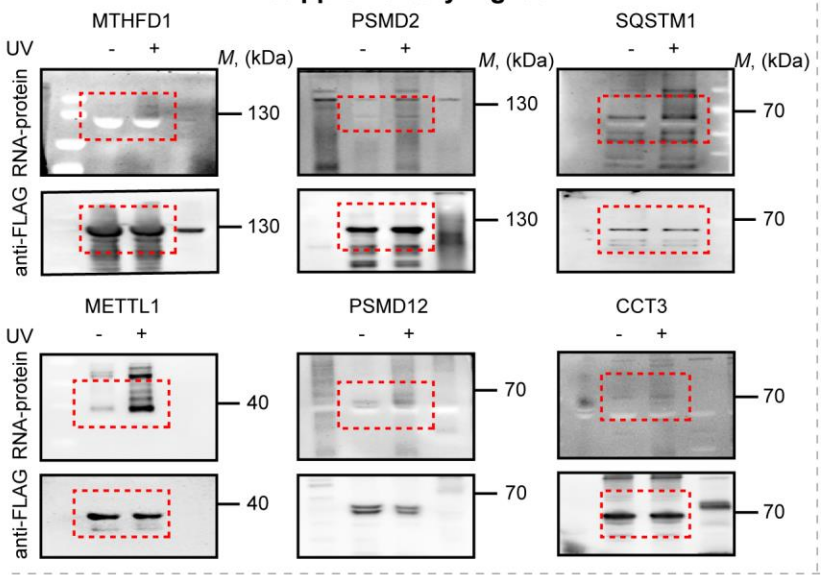

Supplementary Fig. 6c

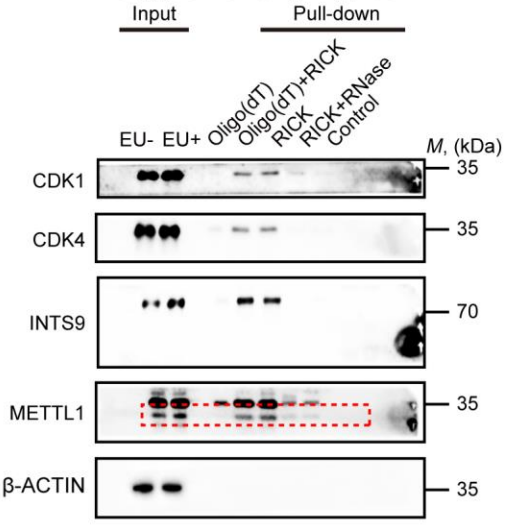

Supplementary Fig. 5f

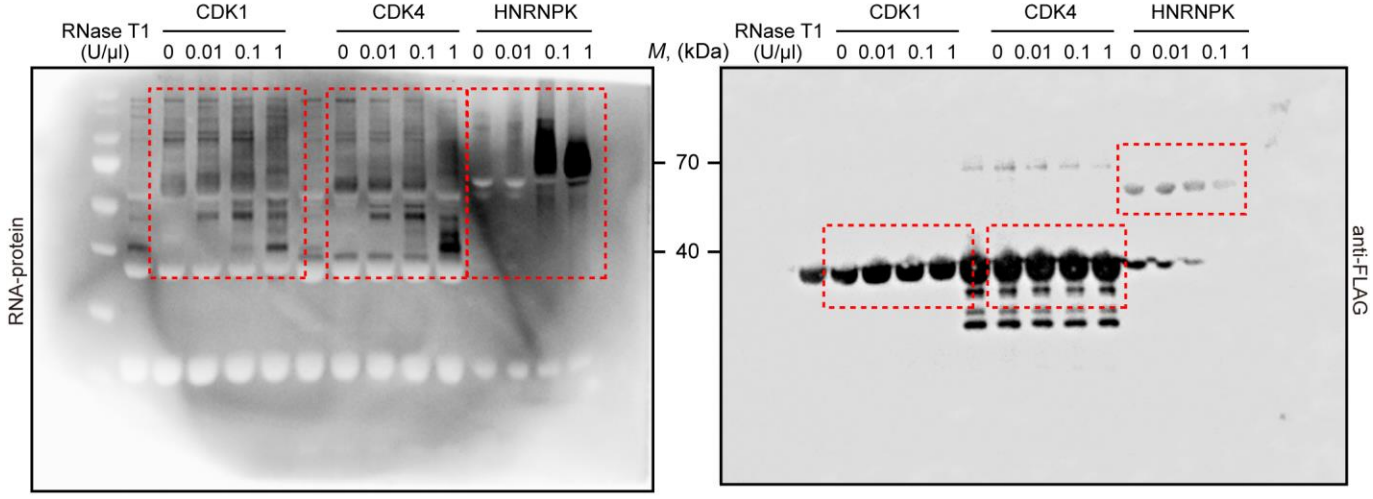

Supplementary Fig. 9b

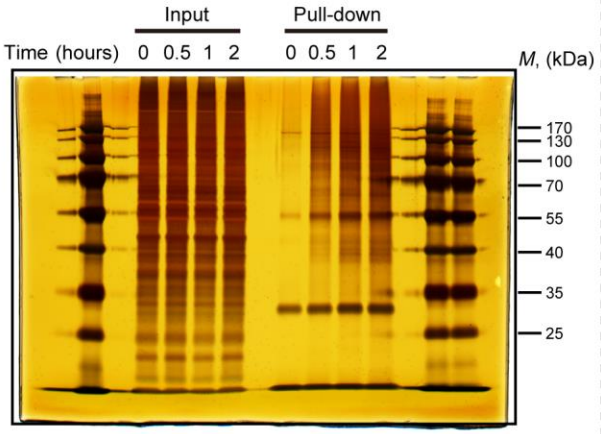

Supplementary Fig. 9e

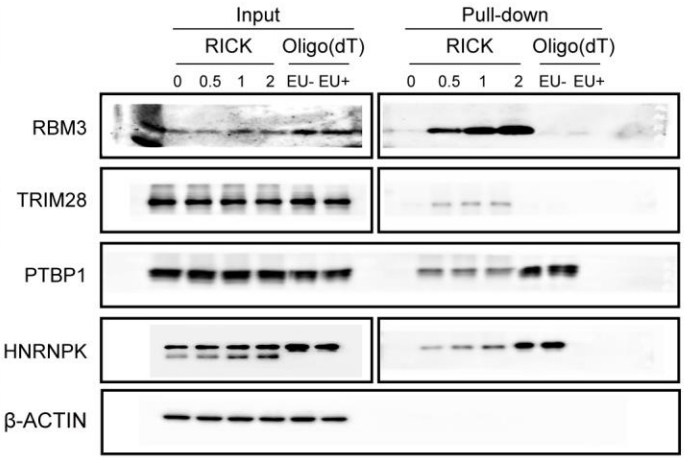

Nature Methods: doi:10.1038/nmeth.4595

Supplementary Figure 12

Raw gels for all figures in the manuscript.

All the gels used in this manuscript have been repeated independently at least 3 times in our laboratory. This figure shows the original scans for all of the representative gels.

Supplementary Note

RICK identifies multiple proteasome complex subunits as candidate RBPs

Sixteen-hour labeling RICK in HeLa cells identified 16 proteasome complex subunits in the high-confidence group (**Supplementary Fig. 5d and Supplementary Table 3a**). In contrast, amongst the different oligo(dT) capture studies in mammalian cells, including our own in HeLa cells, only 3 proteasome subunits were amongst the high-confidence proteins identified by Castello *et al.*[1] and Beckmann *et al.*[2] On the other hand, oligo(dT) capture of *S. cerevisiae* and *C. elegans* identified many proteasome complex subunits[3]. These findings suggest that proteasome complex subunits interact more significantly with non-polyA RNAs than polyA RNAs in mammalian cells. A daring explanation is that during the evolution towards complex species, proteasome subunits acquired the ability to interact with a wider range of RNA species including non-polyA RNAs. The types of non-polyA RNAs interacting with proteasome complex subunits and the consequence of this interaction are yet to be studied. Of note, RICK also identified members of the cullin (e.g., CULLIN1) family, which are involved in ubiquitin conjugation[4] (**Supplementary Table 3a**).

RICK identifies multiple transcriptional regulators as candidate RBPs

We also identified multiple proteins related to chromatin and transcription in the 344 RICK-exclusive RBPs in HeLa cells, compared to the oligo(dT) dataset by Castello *et al.* and our own (**Supplementary Fig. 5c and Supplementary Table 4a**). Amongst other relevant proteins, there were components of the SWI/SNF complex (e.g.,

Nature Methods: doi:10.1038/nmeth.4595

SMARCC1/BAF155), histone demethylases (e.g., KDM1A), components of the mediator (e.g., MED24) and integrator complexes (INTS10), and TRIM28. These findings support the growing evidence that RNA is an active partner in controlling epigenetics rather than a passive bystander[5,6]. Interestingly, TRIM28 regulates Pol II stalling at proximal promoters[7] and RICK samples are enriched in promoter-proximal RNAs, suggesting that both phenomena are connected.

RICK unveils a potential link between nascent RNA transcription and on-site metabolite production

Unexpectedly, application of short labeling RICK for nascent RBP isolation in HeLa cells showed enriched capture of metabolic enzymes/factors (**Supplementary Fig. 9g**). Besides their well-known roles in metabolism, many metabolic enzymes/factors exert unrelated functions[8]. In this regard, some of them localize in the nucleus to provide metabolites for controlling epigenetic marks. For example, Li *et al.* showed that nuclear ACSS2 (acyl-CoA synthetase short-chain family member 2) incorporates acetate to produce acetyl-CoA for histone H3 acetylation at autophagy-related loci[9]. Similarly, Sivanand *et al.* reported that nuclear ACLY (ATP-citrate lyase), which is one of the enzymes/factors identified by short labeling RICK (**Supplementary Fig. 9h and Supplementary Table. 6d, 7**), facilitates homologous recombination by altering histone acetylation at double-strand break sites[10]. However, the potential role of RNA in these processes was unknown. The enriched capture of metabolic enzymes/factors by short labeling RICK raises the possibility that nascent RNAs recruit metabolic

Nature Methods: doi:10.1038/nmeth.4595

enzymes/factors to promote on-site production of key metabolites, modify the epigenome, and thus influence transcription. Future studies are needed to clarify what types of RNAs are bound to these metabolic enzymes/factors and whether and how their interplay impacts transcription.

REFERENCES

1. Castello, A. *et al.* Insights into RNA biology from an atlas of mammalian mRNA-binding proteins. *Cell* **149**, 1393-1406 (2012).
2. Beckmann, B. M. *et al.* The RNA-binding proteomes from yeast to man harbour conserved enigmRBPs. *Nat Commun* **6**, 10127 (2015).
3. Matia-Gonzalez, A. M., Laing, E. E. & Gerber, A. P. Conserved mRNA-binding proteomes in eukaryotic organisms. *Nat Struct Mol Biol* **22**, 1027-1033 (2015).
4. Petroski, M. D. & Deshaies, R. J. Function and regulation of cullin-RING ubiquitin ligases. *Nat Rev Mol Cell Biol* **6**, 9-20 (2005).
5. Bose, D. A. *et al.* RNA binding to CBP stimulates histone acetylation and transcription. *Cell* **168**, 135-149.e122.
6. Sigova, A. A. *et al.* Transcription factor trapping by RNA in gene regulatory elements. *Science* **350**, 978-981 (2015).
7. Bunch, H. *et al.* TRIM28 regulates RNA polymerase II promoter-proximal pausing and pause release. *Nat Struct Mol Biol* **21**, 876-883 (2014).
8. Yang, W. *et al.* PKM2 phosphorylates histone H3 and promotes gene transcription and tumorigenesis. *Cell* **150**, 685-696 (2012).
9. Li, X. *et al.* Nucleus-translocated ACSS2 promotes gene transcription for lysosomal biogenesis and autophagy. *Mol Cell* **66**, 684-697 e689 (2017).
10. Sivanand, S. *et al.* Nuclear acetyl-CoA production by ACLY promotes homologous recombination. *Mol Cell* **67**, 252-265 e256 (2017).

Nature Methods: doi:10.1038/nmeth.4595

Supplementary Table 7 | Metabolic enzymes/factors amongst the 43 nascent-enriched RBPs that are RICK-exclusive compared to different HeLa oligo(dT) capture studies. Eight of 43 proteins are metabolism-related coenzymes/cofactors; main function, localization, and the time points used for identification by short labeling RICK are shown.

Uniprot	Metabolic enzyme/factor	Group	Localization	Main function
P04075	ALDOA (aldolase A)	0.5 h	C	Catalyzes fructose-1,6-bisphosphate to glyceraldehyde 3-phosphate and dihydroxyacetone phosphate
P23526	AHCY (adenosylhomocysteinase)	0.5 h	C	Converts S-adenosylhomocysteine to homocysteine and adenosine
P29401	TKT (transketolase)	0.5/1 h	N	Catalyzes the transfer of sugar phosphates to an aldose acceptor
P07195	LDHB (lactate dehydrogenase B)	0.5/1 h	C	Catalyzes the interconversion of pyruvate and lactate with concomitant interconversion of NADH and NAD+
P00558	PGK1 (phosphoglycerate kinase 1)	0.5/1 h	C, M	Catalyzes 1,3-diphosphoglycerate to 3-phosphoglycerate
P55072	VCP (valosin containing protein)	0.5/1/2 h	N, C	An ATPase enzyme that segregates protein molecules from large cellular structures to facilitate their degradation
P06744	GPI (glucose-6-phosphate isomerase)	2 h	N, C, P	Interconverts glucose-6-phosphate and fructose-6-phosphate
P53396	ACLY (ATP citrate lyase)	2 h	N, C, P	Catalyzes the formation of acetyl-CoA and oxaloacetate from citrate and CoA with a concomitant hydrolysis of ATP to ADP and phosphate

Note: C, cytosol; N, nucleus; M, mitochondria; P, plasma membrane; main function is taken from the NCBI gene database; subcellular localization is taken from either Thul *et al.*, Science, 356, eaal3321 (2017) or Li *et al*., Mol Cell, 61, 705-719 (2016).